Check for updates

RESEARCH ARTICLE

Investigating the effect of electrolyte incorporation on the thermoelectric power factor of bismuth and antimony telluride alloys

[version 1; peer review: 1 approved, 1 approved with reservations, 1 not approved]

Md Mahmudur Rahman[1*], Bejan Hamawandi[2*], Lourdes Márquez-García[1*], Mauricio Solis-de la Fuente[1], Muhammet S. Toprak[2], Jorge García-Cañadas[1]

[1]Department of Industrial Systems Engineering and Design, Universitat Jaume I, Castelló de la Plana, Valencian Community, 12006, Spain
[2]Department of Applied Physics, KTH Royal Institute of Technology, Stockholm, SE10691, Sweden

* Equal contributors

v1 **First published:** 16 Sep 2025, **5**:282
https://doi.org/10.12688/openreseurope.21352.1
Latest published: 16 Sep 2025, **5**:282
https://doi.org/10.12688/openreseurope.21352.1

Abstract

Background

Thermoelectric (TE) devices are capable of converting thermal energy into electrical power. The key parameters to assess the performance of a TE material are the power factor ($PF=S^2\sigma$, S and σ being the Seebeck coefficient and the electrical conductivity, respectively) and the thermal conductivity. In recent years, our group has reported significant *PF* improvements rising from the combination of a porous TE solid with an electrolyte. These results were achieved when Sb-doped SnO_2 was employed as the TE solid. However, due to the modest TE properties of Sb:SnO_2, not very high *PF* values were reached. Here, we evaluate if any *PF* improvements can be reached when electrolytes combine with porous bismuth and antimony telluride alloys, the best-performing TE materials at room temperature.

Methods

Both n-type Bi_2Te_3 and p-type Sb_2Te_3 porous materials were prepared and then combined with different types of electrolytes. Their synthesis was performed by microwave-assisted hydrothermal route, followed by cold compaction of fabricated nanoparticles.

Open Peer Review

Approval Status ? ✗ ✓

	1	2	3
version 1 16 Sep 2025	? view	✗ view	✓ view

1. **Yasuhiro Hasegawa**, Saitama University, Saitama, Japan
2. **Abhigyan Ojha**, Indian Institute of Technology (IIT) Bhubaneswar, Bhubaneswar, India
3. **Oscar Juan Dura**, Universidad de Castilla-La Mancha, Ciudad Real, Spain

Any reports and responses or comments on the article can be found at the end of the article.

Results

Unlike the previous successful results with $Sb:SnO_2$, no significant *PF* improvements were reached in any of the electrolytes tested. This was attributed to the larger carrier concentration and particle dimensions of the bismuth and antimony telluride alloys compared with $Sb:SnO_2$.

Conclusions

Thus, the strategy cannot be extended to bismuth and antimony telluride alloys, and very likely will not work with materials with large carrier concentration.

Keywords
Electrolytes, Bi2Te3, Sb2Te3, hydrothermal, ionic liquid, redox molecule, porous



This article is included in the Horizon 2020 gateway.

Corresponding author: Jorge García-Cañadas (garciaj@uji.es)

Author roles: Rahman MM: Formal Analysis, Investigation, Methodology, Validation, Visualization, Writing – Original Draft Preparation; **Hamawandi B**: Formal Analysis, Investigation, Methodology, Visualization, Writing – Original Draft Preparation; **Márquez-García L**: Investigation, Methodology, Validation; **Solis-de la Fuente M**: Investigation, Methodology, Validation; **Toprak MS**: Conceptualization, Formal Analysis, Funding Acquisition, Methodology, Project Administration, Resources, Supervision, Visualization, Writing – Review & Editing; **García-Cañadas J**: Conceptualization, Formal Analysis, Funding Acquisition, Methodology, Project Administration, Resources, Supervision, Visualization, Writing – Review & Editing

Competing interests: No competing interests were disclosed.

Grant information: This project has received funding from the European Union's Horizon 2020 research and innovation programme under grant agreement No 863222 (UncorrelaTEd project). This was assigned to M. M. Rahman, B. Hamawandi, L. Márquez-García, Mauricio Solis-de la Fuente, Sergio Castro-Ruiz, M. S. Toprak and J. García-Cañadas. Support was also provided by the Conselleria de Educación, Universidades y Empleo of Generalitat Valenciana, under the Santiago Grisolia programme (CIGRIS/2021/072), assigned to M. M. Rahman. Funding is also acknowledged from the Olle Engkvist Foundation (SOEB, 226-0113), assigned to M. S. Toprak.

Copyright: © 2025 Rahman MM *et al*. This is an open access article distributed under the terms of the Creative Commons Attribution License, which permits unrestricted use, distribution, and reproduction in any medium, provided the original work is properly cited.

How to cite this article: Rahman MM, Hamawandi B, Márquez-García L *et al.* **Investigating the effect of electrolyte incorporation on the thermoelectric power factor of bismuth and antimony telluride alloys [version 1; peer review: 1 approved, 1 approved with reservations, 1 not approved]** Open Research Europe 2025, **5**:282 https://doi.org/10.12688/openreseurope.21352.1

First published: 16 Sep 2025, **5**:282 https://doi.org/10.12688/openreseurope.21352.1

Introduction

It is estimated that 72% of the energy consumed globally is wasted as heat[1]. This is such a huge amount that recovering only 10% of this heat would exceed the total energy generated by modern renewable energy sources (wind, solar, geothermal and hydro-energy)[2,3]. Unlike waste heat, omnipresent heat sources including solar radiation and human body heat are widely available. Thus, the conversion of low-grade heat into electricity is something highly desirable and can significantly contribute to mitigating the current energy crisis. In this respect, thermoelectric (TE) devices have drawn significant interest due to their capability to directly convert heat into electricity in an eco-friendly, safe, and silent manner[4,5]. TE technology has already been employed in a variety of applications such as generating power from automotive exhausts, powering instruments for space exploration, recovering heat from industrial furnaces, harnessing solar energy, powering sensors, and many more[4–6].

The heat-to-electricity energy conversion efficiency of a TE material is related to the dimensionless figure of merit $zT=S^2\sigma T/\kappa$, where S is the Seebeck coefficient, σ is the electrical conductivity, T is the absolute temperature, and κ is the thermal conductivity. Thus, large power factor ($PF=S^2\sigma$) as well as low κ are key to obtaining high zT. Most of the recent improvements in the figure of merit have been mainly achieved by reducing κ through approaches including nanostructuring, doping, or defect engineering. Despite this, κ is nearly reaching its amorphous limit in many cases, making necessary to enhance the PF[7,8]. Nevertheless, efforts to increase the PF are limited and challenging due to the adverse correlation between S and σ[9–11].

In recent years, our group has developed a new concept to improve the *PF,* which is based on the interactions of an electrolyte with a porous TE solid. So far, all our studies have employed a porous and nanostructured Sb-doped SnO_2 material as the TE solid. Very large PF improvements (>2.5 times) were obtained in many cases with different electrolytes: a solution of lithium tetrafluoroborate ($LiBF_4$) in 3-methoxypropionitrile (3-MPN)[12], the ionic liquid 1-butyl-3-methylimidazolium iodide (BMII)[12], the redox molecule Cr(III) acetylacetonate dissolved in 3-MPN[13], and the polymer electrolyte poly(diallyldi methylammonium chloride) (PDADMAC)[14]. However, despite the significant PF improvements in Sb:SnO_2, the obtained PF values were far from the state of the art, since Sb:SnO_2 exhibits modest TE properties ($S\approx45$ μV/K).

In this article, we investigate if similar PF enhancements can also be produced in high-performance n- and p-type bismuth and antimony telluride alloys, which are the best-performing TE materials around room temperature[15].

First, we synthesized nanoparticles of n-type Bi_2Te_3 and p-type Sb_2Te_3, which were cold pressed to form pellets with PF values close to the state of the art, while preserving a porous structure. Then, the pellets were brought into contact with several electrolytes to identify if the desired improvements can be reached.

Methods

All chemicals utilized in this study were of analytical grade and sourced from Sigma Aldrich (Stockholm, Sweden). The synthesis process involved bismuth chloride ($BiCl_3$, 98%, ref. 7787-60-2), sodium tellurite (Na_2TeO_3, 99%, ref. 10102-20-2), sodium hydroxide (NaOH, 97.0%, ref. 1310-73-2), and sodium borohydride ($NaBH_4$, 98%, ref. 16940-66-2) as the main reagents. $BiCl_3$ and Na_2TeO_3 were used as sources of Bi and Te ions, respectively. Deionized water served as the solvent, ethylenediaminetetraacetic acid (EDTA, ref. 60-00-4) was used as the shape directing agent, $NaBH_4$ acted as the reducing agent, and NaOH was added to adjust the pH of the reaction medium. The synthesis was conducted using a Milestone flexiWAVE microwave (MW) system 1800 W (Milestone Srl, Sorisole, Italy). Acetone (ref. 67-64-1), and isopropanol (ref. 67-63-0) were also used in the synthesis as received without any further purification.

Synthesis of Bi_2Te_3 and Sb_2Te_3: it was achieved through solution chemical synthesis, adopting the hydrothermal method and MW-assisted heating[16]. The synthetic protocol details are given for the preparation of a 1 g Bi_2Te_3 or Sb_2Te_3 sample, which can be scaled up. A one-pot synthesis method was used by combining all precursor materials in a single reaction vessel. To synthesize Bi_2Te_3 or Sb_2Te_3, a Bi/Sb to Te molar ratio of 2:3 was maintained. The mixture, including $BiCl_3$ (0.79 g) or $SbCl_3$ (0.72 g), Na_2TeO_3 (0.8 g), EDTA (0.6 g), and $NaBH_4$ (0.6 g), was prepared in a 100 mL Teflon-lined reactor, with the pH adjusted to between 10.5 and 11 using (0.2 g) of NaOH. The solutions were stirred magnetically for 30 min to ensure even mixing before MW heating. The temperature was raised to 220 °C for 4 min, then held for 2 min. After the reaction, the system was cooled down to room temperature, causing the product to settle at the bottom and clear phase separation to occur. The powder was collected by centrifugation and washed with isopropanol, acetone, and deionized water. Finally, the powder was dried in a vacuum oven (MSE PRO, MA2015) at 60 °C.

Fabrication of cold-pressed pellets: To have Bi_2Te_3 materials with good TE properties, we fabricated a set of p- and n-type samples by cold pressing at the optimized pressure of 100 MPa. This was performed in order to mainly improve the electrical conductivity of the material and reach closer values to the state-of-the-art bulk bismuth telluride. The prepared Bi_2Te_3 and Sb_2Te_3 (n and p type, respectively) nano powders were then cold pressed using a die with 10 mm × 5 mm × 0.4 mm dimensions (see Figure 1) under equivalent weight for 5 min.

Characterization: X-ray powder diffraction (XRPD) analysis was performed using a Philips PANalytical X'Pert Pro Powder Diffractometer equipped with a copper anode (Cu-Kα1 radiation, λ=1.5406 Å) to identify crystalline phases of TE powders. The measurements employed continuous scan mode, with a step size of 0.10° (2θ) and a scan rate of 0.02°/s. Crystalline phases were determined using High-score Pro software.

The sample's morphology was analyzed with scanning electron microscopy (SEM, FEI Nova 200, Hillsboro, OR, USA).

To prevent charging and enhance image quality, the SEM samples were attached to the holder using copper tape.

PF measurement system: To evaluate the *PF* of the pellets before and after their exposure to different electrolytes, a cell was assembled, composed of soda-lime glasses of 25 mm × 15 mm and 1.8 mm thickness as substrates (Figure 2). The glasses were cleaned before film deposition by means of three sonication steps of 15 min in different media. In the first step, sonication was performed using a soap (Labkem, SOAP-0685K0)/water solution (1:10 v/v). Then, in the second step, distilled water was used to remove excess soap. Finally, isopropanol (Labkem, PROL-P0P-5K0) medium was employed for sonication. After this, substrates were dried under a compressed air flow and treated in a UV ozone cleaner (Ossila, L2002A2-UK) for 20 min. The pellets were first mounted to a glass substrate using a small piece of double-side tape. Subsequently, both ends of the pellet were painted by Ag paint (RS, ref. 186-3600) to establish electric contact (see Figure 2a). To accommodate the electrolyte, a plastic container (frame) was 3D printed and affixed on the top of the pellet using two component Poxipol epoxy (see Figure 2a), which was allowed to cure overnight. The TE measurements with liquid electrolytes were performed in the configuration shown in Figure 2a. In contrast, the polymer electrolyte PDADMAC, which does not require confinement, was directly added on top of the pellet and dried under ambient conditions overnight, as shown in Figure 2b.

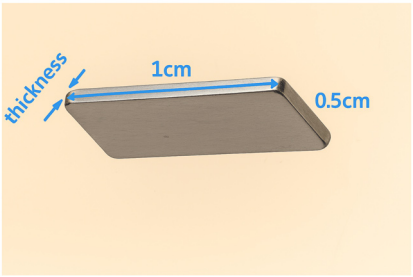


Figure 1. Die. Dimensions of the die for the fabrication of the pellets by cold press.

Electrolytes tested: The different electrolytes that were tested in the n-type Bi_2Te_3 and p-type Sb_2Te_3 samples are listed in Table 1.

Once cells were prepared, Seebeck coefficient and electric resistance (R) were measured before and after the pellets were in contact with the different electrolytes. For each electrolyte two samples were measured to evaluate repeatability when possible. Both S and R were measured in a home-made setup. The Seebeck coefficient was determined by placing the glass substrates with the pellet and the frame (for liquid electrolytes) or only the pellet (for PADAMAC) on top of a small Cu block (30 mm × 30 mm × 10 mm) with 3 inserted cartridge heaters (Watlow, ref. C1E13-L12) that acted as the heat source at the hot side, and on top of a large Cu block (50 mm × 50 mm × 30 mm) that served as heat sink at the cold side, as presented in Figure 2b. Thermal grease (RS, ref. 2173835) was used at the glass/Cu-blocks interfaces to improve the heat transfer. Two K-type thermocouples (RS, ref. 8140134) were positioned on both sides of the pellets to measure the temperature difference ΔT between the hot and cold side (see Figure 2a). These thermocouples were also used to measure the voltage differences, which was recorded using a nanovoltmeter (Keithley 2182A). To determine the Seebeck coefficient, the slope of the ΔT, which was varied from 0 to 5 K in 1 K steps using a PID temperature controller (Watlow EZ-zone), vs the open-circuit potential was calculated. The temperature differences were monitored using a dual datalogger thermometer (RS, ref. 1316). The errors of the measurements, obtained from the fitting error to the linear slope, were below 4%.

R was measured from the slope of current-voltage curves, obtained in a 4-probe mode as illustrated in Figure 2. Two spring probes (RS, ref. 2615092) were positioned on the lateral Ag paint contacts to measure the current. In addition, two similar probes were placed on top of the pellet to measure the voltage. The current was scanned using a Keithley 2450 source meter with a 10 ms delay time. The error of the measurements, determined from the fitting error of the slope, were below 2%. The electrical conductivity $\sigma=L/(RA)$ was then determined using the distance between the voltage probes L,

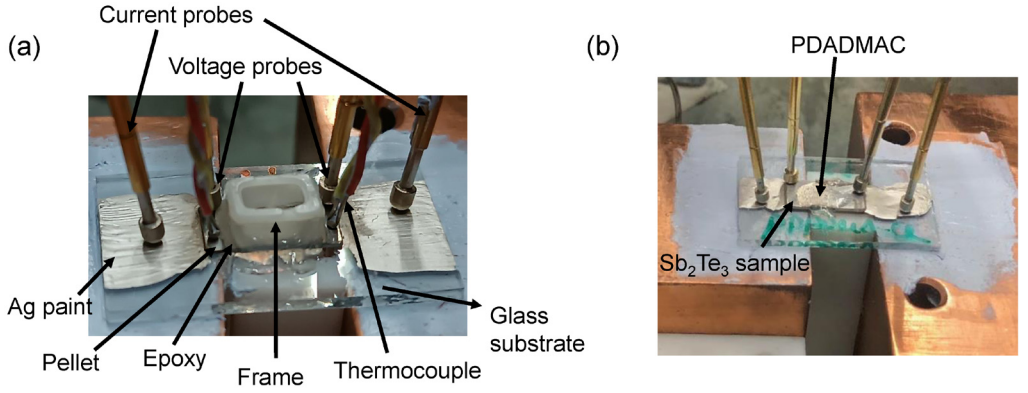


Figure 2. Setups. Setups for the measurement of the pellets in contact with (**a**) liquid electrolytes and (**b**) with the solid electrolyte PDADMAC.

Table 1. Electrolytes. List of the electrolytes tested.

Electrolyte	Type of electrolyte
0.1 M $^{t}BuNH_4BF_4$ (Sigma Aldrich, ref. 217964) in 3-methoxipropionitrile, 3-MPN (Sigma Aldrich, ref. 65290)	Non-electroactive molecule
0.1 M guanidinium chloride (Sigma Aldrich, ref. N018131020 144) in H_2O	Non-electroactive molecule
0.1 M benzoquinone (Sigma Aldrich, ref. B10358-100G) in H_2O	Electroactive (redox) molecule
0.1 M $Cr(acac)_3$ (Sigma Aldrich, ref. 202231) in 3-MPN	Electroactive (redox) molecule
0.1 M $LiBF_4$ (Sigma Aldrich, ref. 244767) in 3-MPN	Non-electroactive salt
0.1 M urea (Sigma Aldrich, ref. U5128-500G) in H_2O	Non-electroactive salt
0.5 mM bis(2-phosphonoethyl) 4,4′-bipyridinium dichloride* in methanol (VWR chemicals, ref. 230526C003)	Electroactive (redox) molecule
1-Butyl-3-methylimidazolium iodide, BMI-I (Solvionic, ref. IM0406C10)	Ionic liquid
1-Ethyl-3-methylimidazolium bis(trifluoromethylsulfonyl)imide, EMIM-TFSI (Solvionic, ref. M0208A10)	Ionic liquid
poly(diallyldimethylammonium chloride) 20 wt.% solution, PDADMAC (Sigma Aldrich, ref. 409022)	Polymer electrolyte

*Compound synthesised as described in ref. 17

and the width and the thickness of the pellets that were used to calculate the cross-sectional area *A*.

Results and discussion

The structure of the synthesized powders was analyzed by XRPD. The XRPD pattern from the Bi_2Te_3 powders in Figure 3a indicates that the powders synthesized through the MW-assisted hydrothermal method have a rhombohedral lattice structure of Bi_2Te_3 space group of R-3m (JCPDS #15-0863). The lattice constants are a=b=4.38 Å and c=30.49 Å, which agree with the reported values (JCPDS #15-0863). The main peaks originated from the (006), (015), (10 10), and (00 15) planes. The sharp diffraction peaks are an indication of the highly crystalline nature of the synthesized Bi_2Te_3 nanostructures.

Figure 3b shows the XRPD pattern of the as-prepared Sb_2Te_3 nanoplates and the diffraction peaks were indexed to the rhombohedral Sb_2Te_3 structure (JCPDS #01-071-0393). No peaks of Te or Sb oxide were detected, indicating the formation of single phase Sb_2Te_3 with a high phase purity. The sharp XRD peaks reveal a high crystallinity in the Sb_2Te_3 nanoplates.

Figure 4a represents the SEM micrograph of the Bi_2Te_3 nanoplatelets, which reveals that the typical powders consist of irregular structures mostly of hexagonal plate-like shapes and nanoparticles. The hexagonal platelets are 300 nm to 1 µm in diagonal and 20–70 nm in thickness, and the nanoparticles are 40–100 nm in diameter. On the other hand, Figure 4b displays the SEM micrographs of the Sb_2Te_3 nanoplatelets showing small and large platelets having edge lengths as small as 80 nm to approximately 1 µm, and thickness ranging from 30 to 120 nm. The presence of micro and nanostructures can provide an improved pathway for the conduction of the charge carriers along the grain boundary.

SEM was also carried out to evaluate the morphology of the prepared pellets. It can be observed from Figure 5 that porosity remains after pressing, since the nanoparticles were not completely compacted. The compaction density of the samples was estimated by taking the ratio of their packing density, calculated from geometrical measurements and mass data, to the theoretical density, from which the porosity was subsequently derived. Porosity values of 41% for Bi_2Te_3 and 32% for Sb_2Te_3 were estimated for the samples pressed at 100 MPa.

The *PFs* of the pellets prepared were measured before and after the exposure to electrolytes. For Bi_2Te_3, the results obtained are shown in Table 2. It can be seen that none of the electrolytes evaluated offered *PF* improvements, since neither the Seebeck coefficient nor the electrical conductivity was significantly affected after the electrolytes were injected.

On the other hand, the results obtained for the Sb_2Te_3 pellets are shown in Table 3. It can be seen again that none of the electrolytes evaluated offered significant *PF* enhancements, since both the Seebeck coefficient and the electrical conductivity were not significantly affected after injecting the electrolytes. We would like to remark that only one measurement per electrolyte was performed in the last electrolytes shown in Table 3 due to the shortage of samples. Finally, we would like to remark that the Seebeck coefficient values in BMI-I and EMIM-TFSI are smaller than in the other electrolytes since their open-circuit voltage were not be measured

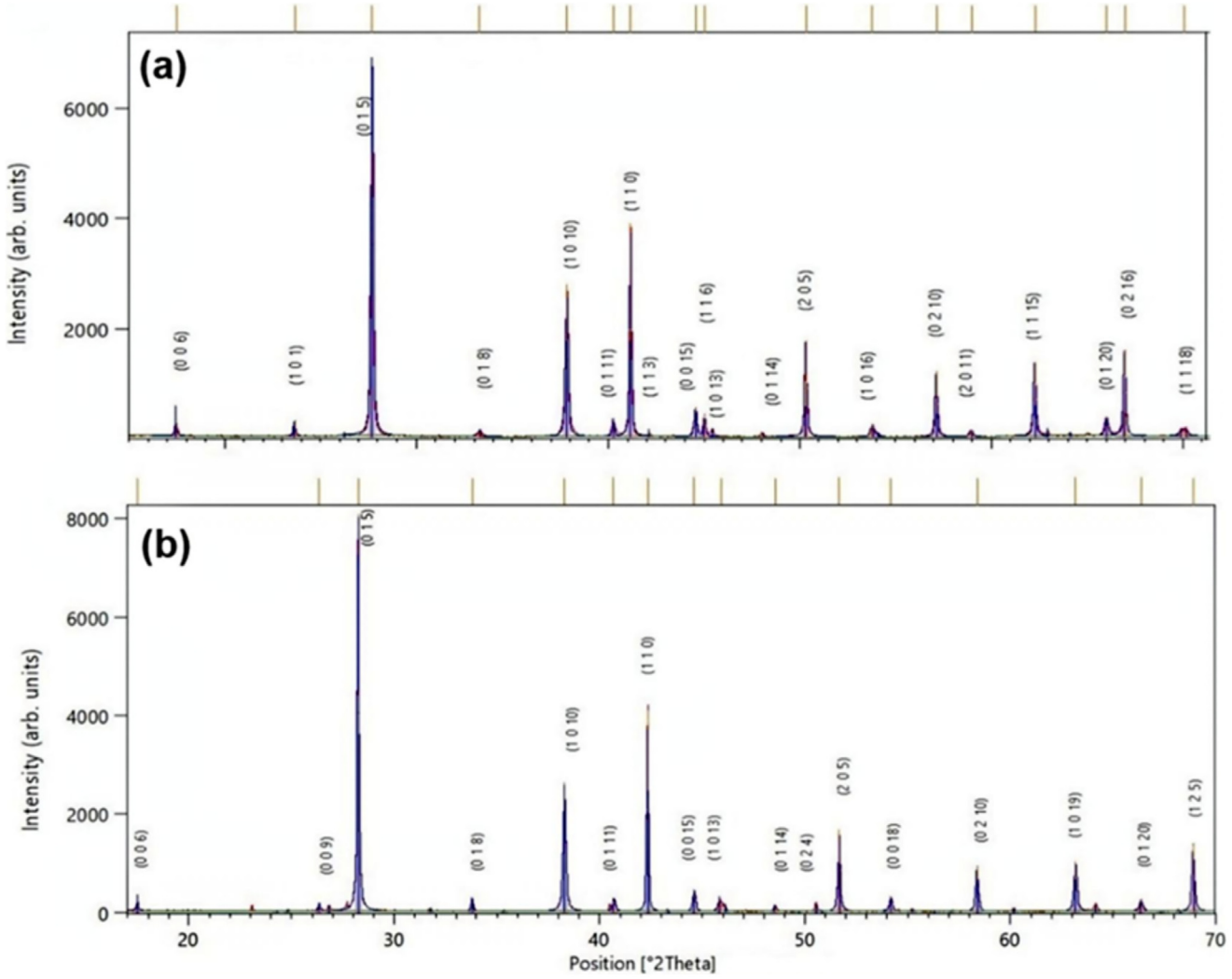


Figure 3. XRPD. XRPD patterns of (**a**) Bi_2Te_3 and (**b**) Sb_2Te_3 nanocrystals synthesized by MW-assisted hydrothermal route. (Peaks are indexed to rhombohedral phase of Bi_2Te_3 with JCPDS #15-0863 and Sb_2Te_3 with JCPDS #01-071-0393).

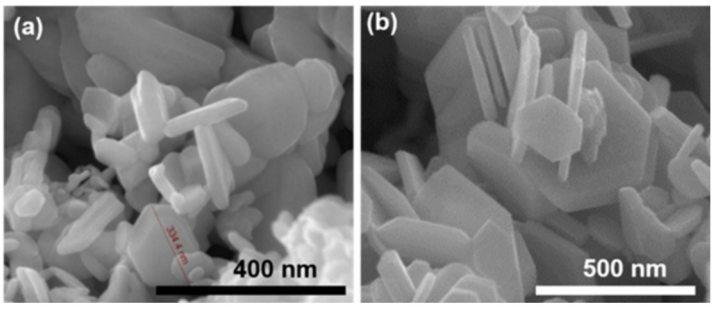


Figure 4. SEM of nanoparticles. SEM micrographs of (**a**) Bi_2Te_3 and (**b**) Sb_2Te_3 nanoplatelets synthesized using MW-assisted hydrothermal route.

with the thermocouples (metal probes were used instead). In spite of this, we decided to include them since measurements are comparative and finally show the *PF* variations.

The observed lack of improvements in the *PF* can be attributed to a higher carrier concentration in the bismuth/antimony telluride alloys and a larger particle size, compared to the

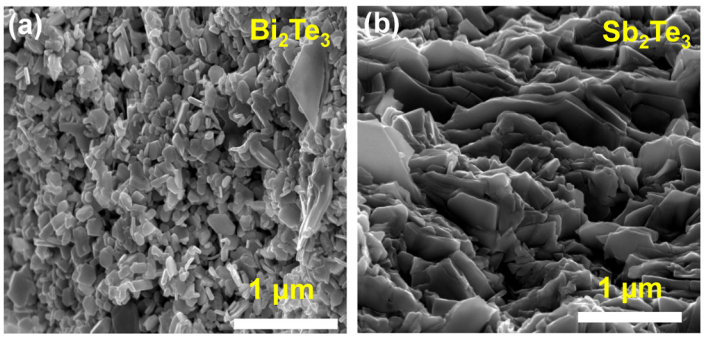


Figure 5. SEM of pellets. SEM images of the cross-sectional view of cold-pressed (**a**) Sb_2Te_3 and (**b**) Bi_2Te_3 pellets compacted at 100 MPa.

Table 2. Power factor of n-type samples. Power factor measurements of Bi_2Te_3 pellets without and with different electrolytes. Results from two different samples are indicated as _1 and _2. The variations in Seebeck coefficient and electrical conductivity, as well as the power factor ratio are given.

Electrolyte	Seebeck coefficient (µV/K)			Electrical conductivity (S/cm)			Power factor ($\mu WK^{-2}m^{-1}$)		
	Without	With	$\lvert\Delta S\rvert$ (%)	Without	With	$\Delta\sigma$ (%)	Without	With	$PF_{with}/PF_{without}$
^{t}BuNH$_4$BF$_4$ _1	-98.08	-101.86	3.85	13.5	13.4	-0.7	12.9	13.9	1.08
^{t}BuNH$_4$BF$_4$ _2	-94.74	-95.71	1.02	13.0	12.6	-3.07	11.6	11.5	0.99
Guanidinium chloride_1	-108.61	-99.95	-8.24	13.3	11.4	-14.3	15.6	11.4	0.73
Guanidinium chloride_2	-98.14	-102.69	4.63	10.6	10.3	-2.91	10.2	10.8	1.06
Benzoquinone_1	-93.43	-95.05	1.73	9.93	10.5	5.74	8.6	9.4	1.09
Benzoquinone_2	-104.17	-103.62	-0.52	10.8	10.3	-4.63	11.7	11.0	0.94
Cr(acac)$_3$ _1	-92.63	-93.57	1.01	14.6	14.2	-2.74	12.5	12.4	0.99
Cr(acac)$_3$ _2	-88.40	-94.76	7.19	17.2	15.9	-7.55	13.4	14.2	1.06

Table 3. Power factor of p-type samples. Power factor measurements of Sb_2Te_3 pellets without and with different electrolytes. Results from two different samples are indicated as _1 and _2. The variations in Seebeck coefficient and electrical conductivity, as well as the power factor ratio are given.

Electrolyte	Seebeck coefficient (µV/K)			Electrical conductivity (S/cm)			Power factor ($\mu W/K^{-2}m^{-1}$)		
	Without	With	$\lvert\Delta S\rvert$ (%)	Without	With	$\Delta\sigma$ (%)	Without	With	$PF_{with}/PF_{without}$
LiBF$_4$_1	162.80	159.05	-2.30	51.5	55.2	6.80	136.0	140.0	1.02
LiBF$_4$_2	155.90	152.61	-2.11	10.4	10.2	-1.77	25.3	23.7	0.94
^{t}BuNH$_4$BF$_4$ _1	153.65	151.70	-1.26	16.2	16.1	-0.61	38.2	37.0	0.97
^{t}BuNH$_4$BF$_4$ _2	153.72	155.48	1.14	18.2	15.7	-13.7	43.0	37.9	0.92
Urea_1	163.14	164.94	1.10	54.5	51.4	-5.68	145.0	139.0	0.96
Urea_2	163.32	163.10	-0.13	40.3	44.1	9.43	107.1	117.0	1.09
Viologen _1	161.08	167.85	4.20	43.6	47.5	8.94	113.2	133.1	1.18
Viologen _1	155.70	154.75	-0.61	18.7	22.0	17.7	45.0	52.1	1.16
PDADMAC	152.17	162.33	6.68	52.39	44.92	-14.3	121.1	118.2	0.92
BMI-I	90.846	83.175	-8.44	30.87	31.07	0.65	25.5	21.5	0.85
EMIM-TFSI	77.566	82.381	6.21	21.95	21.99	0.18	13.2	14.9	1.13

Sb-doped SnO_2 material that showed *PF* improvements above 2.5 times for some of the electrolytes tested here. Nanostructured and porous oxides, such as the Sb:SnO_2 material, typically show an exponential density of states below the conduction band, which is due to a large extent of disorder (e.g. surface and trap states and interparticle boundaries)[18,19]. If the carrier concentration and the particle size is low (e.g. 10^{18}–10^{19} cm^{-3} and 2–40 nm[18,19]), the Fermi level typically lies within this exponential density of states and can move closer to the conduction band when equilibrating with an electrolyte, increasing thus the carrier concentration in the material and hence the electrical conductivity (non-degenerate semiconductor). This occurs because space charges cannot be developed at the surface of the nanoparticles and basically extend to the whole particle (varying the distance of the Fermi level with respect to the conduction band edge, in the case of an n-type material)[20]. This phenomena was observed in our previous studies with Sb:SnO_2[14], that exhibited particle sizes of 4–10 nm.

This equilibration can occur by the formation of a double layer (electrons accumulated in the oxide balanced at the electrolyte part of the interface by cations) and/or by the presence of electroactive species (redox molecules) able to exchange electrons with the oxide. When the carrier concentration of the material is significantly high, the Fermi level no longer falls deep within the exponential density of states but very close or even within the conduction band (degenerate semiconductor). In this case, the equilibration with the electrolyte is achieved by space charges with low penetration inside the nanoparticles (basically at the surface of the oxide) and a significant change in the carrier concentration, and hence, a significant variation in the electrical conductivity of the material, is not possible. In TE materials, such as the bismuth/antimony telluride alloys used in this study, the Fermi level typically lies very close or within the conduction band (for n-type semiconductors) and hence the material is in the degenerate semiconductor situation. In addition, the dimensions of the nanoparticles of the pellets are higher than 2–40 nm (see Figure 5). These factors make difficult to increase the electrical conductivity and hence improve the *PF*.

Conclusions

In this study, we have analyzed the effect of electrolyte integration on the thermoelectric power factor of bismuth/antimony telluride alloys. First, we synthesized nanoparticles of n-type Bi_2Te_3 and p-type Sb_2Te_3 by microwave-assisted hydrothermal route. These were then consolidated by cold pressing to prepare porous pellets, while maintaining good power factor values. Both Bi_2Te_3 and Sb_2Te_3 pellets were brought in contact with different electrolytes, aiming to obtain power factor improvements. No significant variations in the power factors were reached in any of the electrolytes tested. Thus, the strategy of combining thermoelectric solids with electrolytes that produced significant power factor improvements for Sb-doped SnO_2 cannot be extended to bismuth and antimony telluride alloys. This was attributed to the larger carrier concentration and particle sizes in these alloys, when compared to Sb:SnO_2.

Ethics and consent

Ethical approval and consent were not required.

Data availability

Zenodo: Raw data for the article entitled “Investigating the effect of electrolyte incorporation on the thermoelectric power factor of bismuth and antimony telluride alloys”, https://doi.org/10.5281/zenodo.17036143[21].

This project contains the following underlying data:

RawData-XRD.xlsx: This file contains the raw data of Figure 4.

Data are available under the terms of the Creative Commons Attribution 4.0 (CC-BY 4.0).

Acknowledgements

We thank Solvionic for providing the ionic liquids used in this work and for supervising the results obtained.

References

1. Bianchi G, Panayiotou GP, Aresti L, *et al.*: **Estimating the waste heat recovery in the European Union industry.** *Energy Ecol Environ.* 2019; **4**: 211–221.
Publisher Full Text

2. Forman C, Muritala IK, Pardemann R, *et al.*: **Estimating the global waste heat potential.** *Renew Sustain Energy Rev.* 2016; **57**: 1568–1579.
Publisher Full Text

3. Firth A, Zhang B, Yang A: **Quantification of global waste heat and its environmental effects.** *Appl Energy.* 2019; **235**: 1314–1334.
Publisher Full Text

4. Beretta D, Neophytou N, Hodges JM, *et al.*: **Thermoelectrics: from history, a window to the future.** *Mater Sci Eng R Rep.* 2019; **138**: 100501.
Publisher Full Text

5. Champier D: **Thermoelectric generators: a review of applications.** *Energy Convers Manag.* 2017; **140**: 167–181.
Publisher Full Text

6. Ando Junior OH, Maran ALO, Henao NC: **A review of the development and applications of thermoelectric microgenerators for energy harvesting.** *Renew Sustain Energy Rev.* 2018; **91**: 376–393.
Publisher Full Text

7. Wu Z, Zhang S, Liu Z, *et al.*: **Thermoelectric converter: strategies from materials to device application.** *Nano Energy.* 2022; **91**: 106692.
Publisher Full Text

8. Zhou WX, Cheng Y, Chen KQ, *et al.*: **Thermal conductivity of amorphous materials.** *Adv Funct Mater.* 2020; **30**(8): 1903829.
Publisher Full Text

9. Dun C, Hewitt CA, Huang H, *et al.*: **Flexible n-type thermoelectric films based on Cu-doped Bi_2Se_3 nanoplate and Polyvinylidene Fluoride composite with decoupled Seebeck coefficient and electrical conductivity.** *Nano Energy.* 2015; **18**: 306–314.
Publisher Full Text

10. Dehkordi AM, Zebarjadi M, He J, *et al.*: **Thermoelectric power factor: enhancement mechanisms and strategies for higher performance thermoelectric materials.** *Mater Sci Eng R Rep.* 2015; **97**: 1–22.
Publisher Full Text

11. Lin Z, Ping X, Zhao D, *et al.*: **Construct Schottky interface containing energy-filtering effect: an efficient strategy to decouple thermopower and conductivity.** *J Appl Phys.* 2023; **134**(1): 015101.
Publisher Full Text

12. Márquez-García L, Beltrán-Pitarch B, Powell D, *et al.*: **Large power factor improvement in a novel solid-liquid thermoelectric hybrid device.** *ACS Appl Energy Mater.* 2018; **1**(2): 254–259.
Publisher Full Text

13. Castro-Ruiz S, Márquez-García L, Solis-De la Fuente M, *et al.*: **Power factor improvement in a solid-liquid thermoelectric system formed by Sb:SnO_2 in contact with a chromium complex solution.** *Sustain Energy Fuels.* 2023; **7**: 4254–4259.
Publisher Full Text

14. Solis-De la Fuente M, Castro-Ruiz S, Márquez-García L, *et al.*: **Poly(diallyldimethylammonium)-based solid electrolytes to significantly enhance the power factor of a thermoelectric oxide film (Sb-doped SnO_2).** *Sustain Energy Fuels.* 2025; **9**: 1217–1224.
Publisher Full Text

15. Witting IT, Chasapis TC, Ricci F, *et al.*: **The thermoelectric properties of Bismuth Telluride.** *Adv Electron Mater.* 2019; **5**(6): 1800904.
Publisher Full Text

16. Hamawandi B, Batili H, Paul M, *et al.*: **Minute-made, high-efficiency nanostructured Bi_2Te_3 via high-throughput green solution chemical synthesis.** *Nanomaterials (Basel).* 2021; **11**(8): 2053.
PubMed Abstract | **Publisher Full Text** | **Free Full Text**

17. Cummins D, Boschloo G, Ryan M, *et al.*: **Ultrafast electrochromic windows based on redox-chromophore modified nanostructured semiconducting and conducting films.** *J Phys Chem B.* 2000; **104**(48): 11449–11459.
Publisher Full Text

18. Bisquert J, Fabregat-Santiago F, Mora-Seró I, *et al.*: **A review of recent results on electrochemical determination of the density of electronic states of nanostructured metal-oxide semiconductors and organic hole conductors.** *Inorganica Chim Acta.* 2008; **361**(3): 684–698.
Publisher Full Text

19. Fabregat-Santiago F, Mora-Seró I, Garcia-Belmonte G, *et al.*: **Cyclic voltammetry studies of nanoporous semiconductors. Capacitive and reactive properties of nanocrystalline TiO_2 electrodes in aqueous electrolyte.** *J Phys Chem B.* 2003; **107**(3): 758–768.
Publisher Full Text

20. Bisquert J, Garcia-Belmonte G, Fabregat-Santiago F: **Modelling the electric potential distribution in the dark in nanoporous semiconductor electrodes.** *J Solid State Electrochem.* 1999; **3**: 337–347.
Publisher Full Text

21. Hamawandi B, Toprak M: **Raw data for the article entitled "Investigating the effect of electrolyte incorporation on the thermoelectric power factor of bismuth and antimony telluride alloys"**. Zenodo. [Dataset]. (n.d.).
http://www.doi.org/10.5281/ZENODO.17036143

Open Peer Review

Current Peer Review Status: ? ✗ ✓

Version 1

Reviewer Report 28 March 2026

https://doi.org/10.21956/openreseurope.23093.r70811

© **2026 Dura O.** This is an open access peer review report distributed under the terms of the Creative Commons Attribution License, which permits unrestricted use, distribution, and reproduction in any medium, provided the original work is properly cited.

✓ **Oscar Juan Dura**
Universidad de Castilla-La Mancha, Ciudad Real, Spain

The manuscript presents a solid and well-executed study on thermoelectrochemical and thermoelectric systems, clearly reflecting the **strong expertise of the authors** in this field. The work is clearly and accurately presented, and it is supported by an extensive and up-to-date review of the literature, which properly situates the research within a highly active scientific context . The study design is appropriate, and the work undoubtedly holds strong academic merit.
The experimental methodology is particularly noteworthy, combining different characterization techniques within a coherent and multidisciplinary framework. Sufficient details of the methods and analysis are provided, allowing the work to be replicated. In addition, the source data underlying the results appear to be adequately available, ensuring full reproducibility. The conclusions drawn are well supported by the experimental findings presented in the manuscript. The results provide valuable insight about transport properties and performance optimization strategies. However, in the specific case of tellurium-based thermoelectric materials, the approaches explored do not lead to a clear improvement over their performance. While this does not detract from the quality of the research, it somewhat limits its immediate impact in high-performance thermoelectric applications.
Finally, the **manuscript would benefit** from considering the extension of the proposed methodology to alternative material systems. Previous successful results in materials such as SnO_2 suggest that similar strategies could yield more significant improvements, representing a promising direction for future research.

Is the work clearly and accurately presented and does it cite the current literature?
Yes

Is the study design appropriate and does the work have academic merit?
Yes

Are sufficient details of methods and analysis provided to allow replication by others?
Yes

If applicable, is the statistical analysis and its interpretation appropriate?
Yes

Are all the source data underlying the results available to ensure full reproducibility?
Yes

Are the conclusions drawn adequately supported by the results?
Yes

Competing Interests: No competing interests were disclosed.

Reviewer Expertise: Thermoelectricity, transport properties, nanosttructured materials

I confirm that I have read this submission and believe that I have an appropriate level of expertise to confirm that it is of an acceptable scientific standard.

Reviewer Report 08 November 2025

https://doi.org/10.21956/openreseurope.23093.r61576

© 2025 Ojha A. This is an open access peer review report distributed under the terms of the Creative Commons Attribution License, which permits unrestricted use, distribution, and reproduction in any medium, provided the original work is properly cited.

Abhigyan Ojha
Indian Institute of Technology (IIT) Bhubaneswar, Bhubaneswar, Odisha, India

The article titled "Investigating the effect of electrolyte incorporation on the thermoelectric power factor of bismuth and antimony telluride alloys" has been synthesized by the microwave-assisted hydrothermal route, followed by cold compaction of fabricated nanoparticles. The current study exhibited large power factor improvement by employing different electrolytes, as claimed by the author. However, the structure of the current study and the scientific content have a lot of issues in this manuscript. The author suggested doing a major revision for considering the manuscript. Several comments are appended below:

1. Why authors believe that porous structure would be helpful in TE performance, since the core idea of thermoelectrics suggested that the densification of the pellet should be very good to maintain TE performance.

2. Why is such a complex electrolyte chosen rather than some specific one? Mention what the results will be if we use a simple electrolyte NaCl kind of thing. The author is advised to give a detailed explanation regarding the electrolyte chosen.

3. Describe what the major advantage is in the synthesis process employing the hydrothermal route as compared to vacuum sealing or other synthesis routes. The author is suggested to incorporate the detailed explanation of synthesis detail.

4. Why has cold press been employed in the current study rather than hot press? Since the compaction in the hot press is better than the cold press. The author suggested giving a detailed comparison of these two in the context of the current study.

5. In Table 3, the electrical conductivity of the samples seems to be very low. How are the authors defending this observation?

6. The author claims that the strategy of combining thermoelectric solids with electrolytes that produced significant power factor improvements for Sb-doped SnO_2 cannot be extended to bismuth and antimony telluride alloys. In what context do these electrolytes play a superior role?

These are the major comments; besides these, there is a lot of scientific content missing. It is advised to do major correction.

Is the work clearly and accurately presented and does it cite the current literature?
Partly

Is the study design appropriate and does the work have academic merit?
Partly

Are sufficient details of methods and analysis provided to allow replication by others?
Partly

If applicable, is the statistical analysis and its interpretation appropriate?
Partly

Are all the source data underlying the results available to ensure full reproducibility?
No

Are the conclusions drawn adequately supported by the results?
No

Competing Interests: No competing interests were disclosed.

Reviewer Expertise: Energy Materials, Thermoelectric Materials and Devices, Energy Harvesting Materials

I confirm that I have read this submission and believe that I have an appropriate level of expertise to state that I do not consider it to be of an acceptable scientific standard, for reasons outlined above.

Reviewer Report 25 September 2025

https://doi.org/10.21956/openreseurope.23093.r60770

© 2025 Hasegawa Y. This is an open access peer review report distributed under the terms of the Creative Commons Attribution License, which permits unrestricted use, distribution, and reproduction in any medium, provided the original work is properly cited.

?

Yasuhiro Hasegawa
Saitama University, Saitama, Japan

This study investigates materials designed to improve the power factor by employing a porous structure, and examines the potential enhancement of performance by introducing electrolytes into the porous structure. The results indicate, unfortunately, that this approach is not applicable to bismuth and antimony telluride alloys. While the report has significance, the overall presentation contains many parts that are difficult to understand, and it is recommended that the manuscript be rewritten to be clearer for readers.

Although the fabrication method is described, Figure 1 shows only a die, and there is no illustration of the prepared sample, making it difficult to comprehend. Similarly, Figure 2 depicts only the setup after assembly, which may be unclear to first-time readers. It would be helpful to illustrate the sample setup step by step. In particular, while the text mentions that the electrolyte is introduced into the porous structure, this is difficult to grasp from the text alone.

Table 1 lists information about the electrolytes, but it becomes difficult to distinguish them in subsequent figures and text. It is recommended to use labels such as Electrolyte A, B, C, etc., to improve clarity.

The methods for measuring resistance and Seebeck coefficient are simple and standard. However, to demonstrate the reliability of the measurements, it would be clearer to provide an example of the actual data. Descriptions in the text alone are insufficient. Additionally, measurement conditions, such as the fact that the measurements were conducted in air, should be explicitly stated.

Figure 3 confirms that the prepared Bi_2Te_3 and Sb_2Te_3 powders are polycrystalline. Small peaks are also observable, so it would be clearer to use a logarithmic scale on the vertical axis and extend lines near the XRD patterns to indicate the JCPDS reference data. If possible, the crystallite size could also be estimated from the XRD peak widths in conjunction with Figure 4. The porosity of the samples was calculated from their shape and weight, yielding relatively small values of 41% for Bi_2Te_3 and 32% for Sb_2Te_3. It would be helpful to indicate whether these values correspond to the results shown in Figure 5.

Tables 2 and 3 present results but are difficult to read. For example, plotting the Seebeck coefficient on the horizontal axis and the resistivity on the vertical axis, and illustrating how the data shifted before and after electrolyte exposure, would improve clarity.
Various possible reasons for the lack of power factor improvement are discussed. While these possibilities are plausible, there is currently insufficient qualitative or quantitative evidence. If high carrier concentration is suspected as a cause, additional experiments such as Hall measurements to estimate carrier density would be necessary. At this stage, it is important to clearly distinguish between what can be stated with certainty and what remains a possibility.

Is the work clearly and accurately presented and does it cite the current literature?
No

Is the study design appropriate and does the work have academic merit?
Partly

Are sufficient details of methods and analysis provided to allow replication by others?
No

If applicable, is the statistical analysis and its interpretation appropriate?
I cannot comment. A qualified statistician is required.

Are all the source data underlying the results available to ensure full reproducibility?
No source data required

Are the conclusions drawn adequately supported by the results?
Partly

Competing Interests: No competing interests were disclosed.

Reviewer Expertise: The data are not well organized and need to be visualized in a way that is easier for readers to understand.

I confirm that I have read this submission and believe that I have an appropriate level of expertise to confirm that it is of an acceptable scientific standard, however I have significant reservations, as outlined above.